Density Functional Theory Study on the Electronic Structure and Optical Properties of Sb-doped SnO_2

Shao Tingting Zhang Fuchun Cui Hongwei

College of Physics and Electronic Information, Yan'an University, Yan'an, Shaanxi 716000, *China*

Abstract The electronic structures and optical properties of Sb-doped SnO_2 are studied by first principle calculation based on density functional theory (DFT). The computed results show that, with the increase of Sb doping concentration, the Fermi energy level passes through conduction band, and the band gap is narrower in succession, meanwhile, the energy level of shallow donor impurity is shifted away from the conduction band bottom, which makes the conductivity enhanced. The calculated results of charge density indicate that Sb-doping can change the property of SnO_2 bond formation, which makes the covalent weakened and the metallicity enhances with the increase of Sb doping concentration. The calculated results of optical properties show that the imaginary part of the dielectric function has a red shift like the total density of state (TDOS) with the increase of Sb doping concentration, which indicates the internal relationship between electronic structure and optical properties theoretically.

Key words materials; SnO_2; Sb-doping; density functional theory; electronic property; optical property

OCIS codes 160.4236; 160.4760; 160.6000

Sb掺杂SnO_2的电学性质和光学性质密度泛函理论研究

邵婷婷 张富春* 崔红卫

延安大学物理与电子信息学院, 陕西 延安 716000

摘要 基于平面波赝势密度泛函理论,采用局域密度近似(LDA)方法研究了Sb掺杂SnO_2的电子结构和光学性质。计算结果表明,与本征SnO_2比较,Sb掺杂SnO_2的性质,包括能带结构、态密度、电荷密度及光学性质等均随Sb的掺杂浓度变化。Sb掺杂相比本征SnO_2的带隙要窄,带隙随Sb掺杂浓度的增加逐渐变窄,并且浅施主杂质能级逐渐远离导带底。Sb掺杂改变了SnO_2可成键性质,随着掺杂浓度的增加,共价性减弱,金属性增强。光学性质计算结果显示随着掺杂浓度的增加,态密度和介电函数虚部向低能方向移动,发生了明显的红移现象,这从理论上揭示了电子结构和光学性质之间的内在关系。

关键词 材料; SnO_2; Sb掺杂; 密度泛函理论; 电学性质; 光学性质

中图分类号 O471.4 **文献标识码** A

doi: 10.3788/LOP52.081601

1 Introduction

Stannic oxide (SnO_2), an n-type wide band-gap semiconductor, whose experimental band gap is 3.6 eV , has high exciton binding energy (130 meV in experiment)[1]. The new materials formed by doped SnO_2 have higher conductivity and better optical transmittance, and the research on metallic ion doped SnO_2 compound has involved some electronic and optical theories and experimental discusses. Du et al[2] calculated the electronic properties of III family doped SnO_2. Yu et al[3-4] studied the density of states and optical properties of Al, N doped SnO_2. Lu et al[5] investigated the electronic structure and optical properties of Fe-

收稿日期: 2015-02-12; **收到修改稿日期**: 2015-03-31; **网络出版日期**: 2015-07-28

基金项目: 陕西省自然科学基础研究计划(2014JM2-5058)、陕西省教育厅科学研究计划项目(2013JK0917)、延安市科学技术研究发展计划(2013KG-03,2014KG-02)

作者简介: 邵婷婷(1982—),女,硕士研究生,讲师,主要从事纳米材料光电性质方面的研究。E-mail: retastt@126.com

导师简介: 张富春(1972—),男,博士,副教授,主要从事纳米材料光电磁性质方面的研究。

E-mail: zhangfuchun72@163.com(通信联系人)

doped SnO_2.

Stannic oxide conductive film SnO_2: Sb (ATO) has similar photoelectric properties with In_2O_3: Sn (ITO), whose research is mature, and ATO reserve is rich and low cost, so there are many studies about laboratory preparation and process improvement of ATO[6-8]. Guo et al[9] studied the electrical and optical properties of sol-gel processing Sb-doped SnO_2 thin film by experimental measurement. Wang et al[10] prepared SnO_2 B Sb thin films and studied its photoluminescence characteristics. Wang et al[11] prepared SnO_2: Sb transparent conducting thin films by sol-gel method and studied its photoelectric properties. Deng et al[12] investigated the effect of Sb doping on electrical conductivity of SnO_2 by first-principle calculation. However, the reports about first principle simulative calculation of electronic and optical properties of Sb-doped SnO_2, especially high Sb doping concentration, are still not overall. Thus in this paper, we calculate the structural, electronic, and optical properties of different high concentration Sb-doped SnO_2 based on density functional theory (DFT) and analyze the results, which is expected to provide some theory evidence of doping modification about ATO.

2 Calculated methods and theoretical descriptions

2.1 Calculated methods

The theoretical calculations are processed by plane wave pseudo potential method based on the density functional theory[13]. The pseudo-potentials are used to replace ionic potentials, and the electronic wave function is expanded by plane wave basis sets. The electron-electron exchange and associate potential are corrected by the local density approximation (LDA), which is an accurate theory method of electronic structure calculation[14]. The electronic, optical properties of intrinsic and Sb-doped SnO_2 super cell are calculated through the vienna ab-initio simulation package (VASP) program[15]. As shown in Fig.1, the SnO_2 2×2×2 super cell contain 16 Sn atoms and 32 O atoms and the number of Sb to replace Sn is 1-3, whose doping concentration is x=6.25%, x=12.5% and x=18.75% correspondingly. In the calculation, the experimental lattice constant of SnO_2 is taken, that is, a=b=0.4737 nm, c=0.3186 nm, α=β=γ=90°[16]. The energy cut-off of plane wave takes 380 eV, while Monkhorst - Pack mesh of Brillouin-Zone sampling takes 6×6×4, and the self-consistent convergence of the total energy takes 5×10^{-7} eV/atom for intrinsic and Sb-doped SnO_2 super cells. The atomic configuration for O, Sn and Sb are $2s^2 2p^4$, $5s^2 5p^2$ and $5s^2 5p^3$, respectively. For intrinsic SnO_2, the net charge between Sn atom and Sn atom is all 0.58 e, and the net charge between O atom and Sn O is all -0.29 e, which means that same atoms are equivalent.

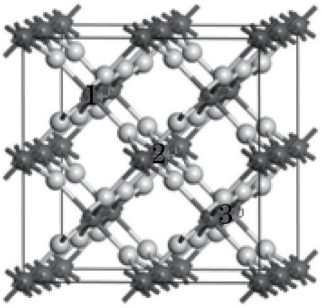

Fig.1 SnO_2 2×2×2 super cell (black ball is Sn atom, grey ball is O atom, the Sn of position 1-3 is substituted for Sb)

2.2 Theoretical descriptions

The complex dielectric function $\varepsilon(\omega)=\varepsilon_1(\omega)+i\varepsilon_2(\omega)$, which can reflect band structure and other spectrum information, is usually used to describe the optical properties of solidity macroscopically. Where $\varepsilon_1=n^2-k^2$, $\varepsilon_2=2nk$ and n is the reflection coefficient, k stands for the extinction coefficient[17]. The real part can be obtained by Kramer-Kroing dispersion relation and imaginary part can be obtained by momentum matrix elements of wave function between occupied states and unoccupied states[18-19].

The derivation process is ignored, and only giving the results.

$$\varepsilon_1(\omega)=1+\frac{8\pi^2e^2}{m^2}\sum_{V,C}\int_{BZ}d^3k\frac{2}{2\pi}\frac{\left|eM_{CV}(K)\right|^2}{\left[E_C(K)-E_V(K)\right]}\times\frac{h^3}{\left[E_C(K)-E_V(K)\right]^2-h^2\omega^2}, \tag{1}$$

$$\varepsilon_2(\omega)=\frac{4\pi^2}{m^2\omega^2}\sum_{V,C}\int_{BZ}d^3k\frac{2}{2\pi}\left|eM_{CV}(K)\right|^2\times\delta\left[E_C(K)-E_V(K)-h\omega\right], \tag{2}$$

$$I(\omega)=\sqrt{2}(\omega)\left[\sqrt{\varepsilon_1(\omega)^2-\varepsilon_2(\omega)^2}-\varepsilon_1(\omega)\right]^{1/2}, \tag{3}$$

$$R(\omega)=\frac{(n-1)^2+k^2}{(n+1)^2+k^2}, \tag{4}$$

Where C, V is conduction band and valence band, BZ is first Brillouin-zone, ω is light frequency, K is reciprocal vector, $\left|eM_{CV}(K)\right|^2$ is momentum transition matrix element. The above equations are the theory evidences of analyzing crystal band structure and optical properties. It reflects the luminescence mechanism generated by the electronic transitions between the energy levels.

3 Results and discussion

3.1 Electronic properties

As mentioned in paper[20], when the order of magnitude of doping concentration is lower than 10^{18} cm^{-3}, the situation is considered as low doping, and that regards as high doping when the order of magnitude is equal or greater than 10^{18} cm^{-3}. The Sb-doped SnO_2 are all high doping, and the result of Fermi level goes into the conduction band in the latter analysis further proved that.

The energy band structures of intrinsic SnO_2 and Sb-doped SnO_2 are shown in Fig.2.

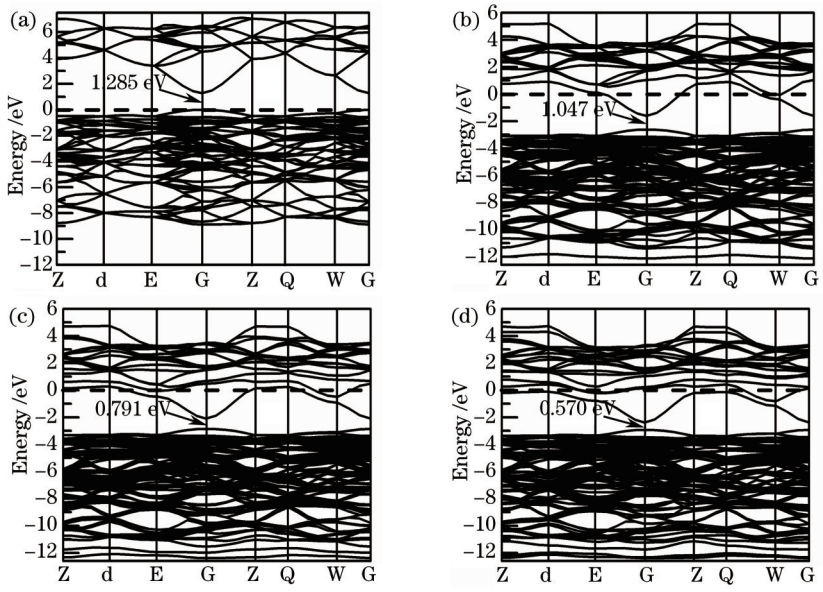

Fig.2 Calculated band structure of Sb-doping SnO_2. (a) x=0%; (b) x=6.25%; (c) x=12.5%; (d) x=18.75%

From the Fig.2, it can be seen that the Sb-doped SnO_2 is direct band-gap semiconductor like intrinsic SnO_2. The Fermi level is chosen to be zero of the energy scale, and the occupied state below the Fermi energy is valence band, whereas the unoccupied state lying above the Fermi energy is conduction band. The position of bottom of conduction band and top of valence band is G-point of Brillouin zone. The band gap are 1.285 eV, 1.047 eV, 0.791 eV, 0.570 eV for x=0%, x=6.25%, x=12.5% and x=18.75% Sb doping concentration of SnO_2, respectively, which are all lower than available experimental data (3.7~3.8 eV) mentioned in this paper[9]. This is because LDA is ground state theory, and the energy-gap belongs to property of excited state[21]. The calculated band gap of intrinsic SnO_2 is closed to the calculated result 1.3 eV of paper[5], which

proves that the method and adopted process are right. In order to make the band gap approach the experimental data, the scissors are set to 2.4 eV in the later optical properties calculation.

The band gap of Sb-doped SnO_2 is reduced in succession with the increase of Sb doping concentration, and the Fermi energy level moves into the conduction band. Compared intrinsic SnO_2, the amount of energy level of Sb-doped SnO_2 obviously increase, especially in the valence band, which means that the number of transition electrons between energy level increase. Therefore, the conductivity of Sb- doped SnO_2 improves. The energy level of conduction band is winding and overlap with the increase of Sb doping concentration, because there are great number of surplus electrons at the bottom of conduction band when the Fermi level goes into the conduction band. According to the theoretical analysis of renormalization, that is mainly because the high Sb doping concentration makes free charges changed the band gap of SnO_2 in two aspects. In one hand, high Sb doping concentration brings Burstein-Moss movement, and the edge of optical absorption moves to low energy direction, which lead to widening band gap. On the other hand, the interactions among charges makes multi-body effect or overlapping between impurity band and defect band, which makes the band gap narrow. The two aspects compete with each other, and with the increase of Sb doping concentration, Burstein-Moss effect is less than multi-body effect, so for high Sb doping SnO_2, the more concentration the narrower band gap.

The total density of state (TDOS) and partial density of states (PDOS) of intrinsic SnO_2 and Sb-doped SnO_2 are shown in Fig.3.

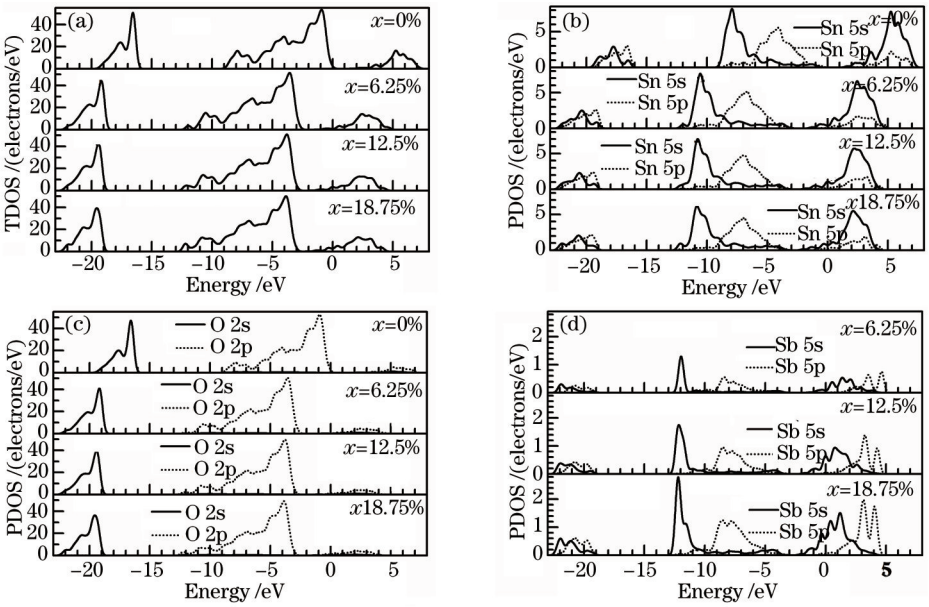

Fig.3 Calculated TDOS and PDOS for x=0%, x=6.25%, x=12.5% and x=18.75% Sb doping concentration of SnO_2 (a) TDOS; (b) Sn 5s, Sn 5p PDOS; (c) O 2s, O 2p PDOS; (d) Sb 5s, Sb 5p PDOS

From the Fig.3, it is found that TDOS of Sb-doped SnO_2 has a red shift with the decrease of band gap and the positions of peak values are mainly identical. From the Figure of density of state of 6.25% Sb-doped SnO_2, we can find that the valence band includes two parts, the low valence band, $-22.5\sim-13.0$ eV region, which is dominated by O $2s^2$ states, with a minor-presence of Sn $5s^2$, Sn $5p^2$, Sb $5s^2$ and Sb $5p^3$ states, which can be ignored because it is far from Fermi level that has little influence with it. The high valence band can be divided into two sections, $-13.0\sim-9.5$ eV region is dominated by Sn $5s^2$ and Sb $5s^2$ states, which raise with the increase of Sb doping concentration, and $-9.5\sim0$ eV region, which is closed to Fermi level, is dominated by O $2p^4$ and Sn $5p^2$ states, with a few contributions of Sb $5p^3$ states which still enhance with the increase of Sb doping concentration. It illustrates that O atom can absorb electrons strongly from Sb atom and Sn atom. The conduction band is mainly dominated by Sn $5p^2$, Sn $5s^2$, Sb $5s^2$ and Sb $5p^3$, and O $2p^4$ have a few

contributions. Combined the TDOS, PDOS and the energy band structure, there is a about 1 eV -width band at the 12 eV point, which is mainly caused by Sb $5s^2$, and with the increase of Sb doping concentration, the width broaden.

Figure.3 (a) shows that the TDOS of Sb-doped SnO_2 at Fermi level is affected by Sb doping, and the influence strengthens with the increase of Sb doping concentration, which also influences the optoelectronic properties of SnO_2 materials. The electrons at Fermi level distribute asymmetrically and Sb- doped SnO_2 materials present half- metallic property, which mainly due to Sb $5s^2$ states and is corresponding to the increasing number of energy levels at Fermi level towards Brillouin zone in the energy band structure Figure. Meanwhile, the total density of state shift towards low energy direction with the increase of Sb doping concentration, which mainly lead to Fermi level going into conduction band and making the band gap narrower.

For intrinsic SnO_2, from Fig.3 (b),(c), it is found that Sn-5*s* and O-2*p* orbital electrons interact to form anti-bonding-like state of *s* orbital and bonding state of *p* orbital, which produce band gap. For Sb-doping SnO_2, as shown in Fig.3 (b)~(d), at the bottom of conduction band, Sb-5*p* orbital electrons has lower energy than Sn-5*s*, and Sb-5*p* and O-2*p* orbital electrons form anti-bonding-like state of *p* orbital, which has lower energy than anti-bonding-like state of *s* orbital in intrinsic SnO_2. Sb-5*p* orbital moves to low energy that leads to the descending of conduction band. With the increase of Sb high doping concentration, the movement towards low energy and the conduction band descending are all more obvious. In addition, the *p*-*p* orbital interaction makes valence band moving to low energy, and *p*-*d* repelling effect causes valence band moving to high energy. From the calculated results, it can be seen that with the increase of Sb high doping concentration, *p*-*p* interaction is stronger than *p*-*d* repelling effect, and the valence band descends more. However, with the increase of Sb high doping concentration, the conduction band is descending more than valence band, so the band gap is narrower.

3.2 Charge density

The charge density in the (1 1 1) basal plane for of intrinsic SnO_2 and Sb-doped SnO_2 are shown in Fig.4.

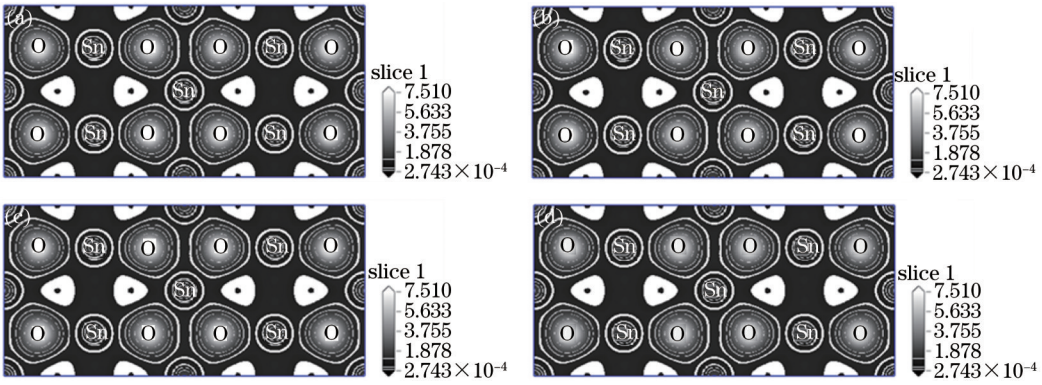

Fig.4 Calculated total charge density of different Sb-doping concentration SnO_2.

(a) x=0%; (b) x=6.25%; (c) x=12.5%; (d) x=18.75

Figure 4 shows that there are great atomic bonding properties differences between intrinsic SnO_2 and Sb- doped SnO_2, and the charge is redistributed. For intrinsic SnO_2, Sn atoms and O atoms form covalent bond, which contain ionic bond. However, for Sb-doped SnO_2, the charge distribution of atoms around doped Sb is effected and the electron communization improves. With the increase of Sb doping concentration, the ionicity enhances. Sb atoms and O atoms around it form overlapping regions of charge density, and the overlapping strengthens with the Sb- doping concentration increased. As a whole, electrons gather from Sb atoms to O atoms.

3.3 Optical property

The experimental result of Ref.[10] shows that Sb-doped SnO_2 has (1 1 0) preferred orientation, so the complex dielectric functions of intrinsic SnO_2 and Sb-doped SnO_2 from the polarization vectors (1 1 0) are calculated, and they are shown in Fig.5.

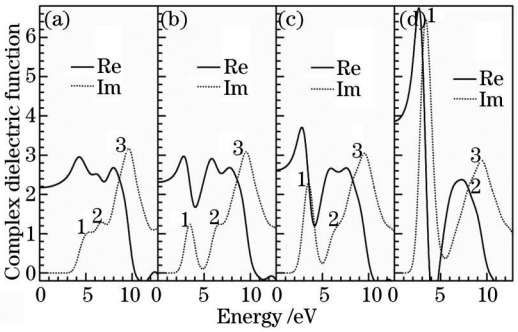

Fig.5 Calculated complex dielectric function of different Sb-doping concentration SnO_2.
(a) x=0%; (b) x=6.25%; (c) x=12.5%; (d) x=18.75%

From the Fig.5, we can see that the real part $\varepsilon_1(\omega)$ is descended as a whole as the energy increases, and the intensity reaches maximum at 4.28 eV, 2.75 eV, 2.83 eV, 2.65 eV for x=0%, x=6.25%, x=12.5% and x=18.75% Sb doping concentration of SnO_2. The probability of photon absorption is directly related to the imaginary part of complex dielectric function $\varepsilon_2(\omega)$. For $\varepsilon_2(\omega)$, the points of curves beginning to rise are very consistent with the calculated energy gaps which add scissors, and there are three main transition peaks at the low energy region. The peaks appear because of the electrons transition from valence band to conduction band. The position of first peak is wide, which is about 3.39~5.08 eV, and the peak value increases with the increase of Sb doping concentration. The first peak arises from O $2p^4$ orbits to Sn $5s^2$ orbits, and some arise from Sb $5s^2$ orbits to Sn $5s^2$ orbits for Sb-doped SnO_2. The second peak is at about 6.50 eV, which mainly results from O $2p^4$ orbits to Sn $5p^2$ orbits, and some arise from Sb $5s^2$ orbits to Sn $5p^2$ orbits for Sb-doped SnO_2. The third peak, whose position is at about 9.56 eV, appears because of O $2s^2$ orbits to Sn $5s^2$ orbits, and some arise from Sb $5p^3$ orbits to Sn $5p^2$ orbits for Sb-doped SnO_2, and the peak value gradually reduces with the increase of Sb doping concentration. The more Sb doping concentration, the higher transition peak, which because Sb $5p^3$ state and O $2p^4$ state have strong coupling and lead to the changing of impurity level in the band gap. With the increase of Sb doping concentration, the transition peaks have a red shift towards low energy direction as a whole, and that is in accord with the previous calculated band gap, which is reduced with the Sb-doping concentration increased.

4 Conclusion

In conclusion, the electronic structures and optical properties of Sb-doped SnO_2 by plane-wave pseudopotential DFT with LDA are studied. The band gap for x=0%, x=6.25%, x=12.5% and x=18.75% Sb doping concentration of SnO_2 is narrower in succession and the Fermi level moves into conduction band gradually. According to the theoretical analysis of renormalization and orbital theory, the reason of above calculated results is analyzed. With the increase of Sb doping concentration, the bond property changes and the ionicity enhances. The total density of states and imaginary part of the dielectric function has a red shift with the decrease of band gap, and the transition peaks have relationship with the electrons absorption from valence band to conduction band.

References

1 Batzill M, Katsiev K, James M, *et al*.. Gas-phase-dependent properties of SnO_2 (110), (100), and (101) single-crystal surfaces: Structure, composition, and electronic properties[J]. Phys Rev B, 2005, 72(1): 165414-20.

2 Du Juan, Ji Zhenguo. The effect of III-family element doping on electronic structures and electrical characteristics of SnO_2[J]. Acta Phys Sin, 2007, 56(4): 2388-2392.
杜 鹃, 季振国. III族元素掺杂对SnO_2电子结构及电学性能的影响[J]. 物理学报, 2007, 56(4): 2388-2392.
3 Yu Feng, Wang Peiji, Zhang Changwen. Electronic structure and optical properties of Al-doped SnO_2[J]. Acta Phys Sin, 2011, 60(2): 023101.
于 峰, 王培吉, 张昌文. Al掺杂SnO_2材料电子结构和光学性质[J]. 物理学报, 2011, 60(2): 023101.
4 Yu Feng, Wang Peiji, Zhang Changwen. First-principles study of optical and electronic properties of N-doped SnO_2[J]. Acta Phys Sin, 2010, 59(10): 7285-7290.
于 峰, 王培吉, 张昌文. N掺杂SnO_2材料光电性质的第一性原理研究[J]. 物理学报, 2010, 59(10): 7285-7290.
5 Lu Yao, Wang Peiyi, Zhang Changwen, *et al*.. First-principles calculation on electronic structure and optical properties of iron-doped SnO_2[J]. Acta Phys Sin, 2011, 60(11): 1131901.
逯 瑶, 王培吉, 张昌文, 等. 第一性原理研究Fe掺杂SnO_2材料的光电性质[J]. 物理学报, 2011, 60(11): 113101.
6 Zhang Zhiguo. Variable gap and gap state distribution of film silicon[J]. Acta Phys Sin, 2008, 62(14): 147301.
张治国. 薄膜硅的变隙问题及隙态分布[J]. 物理学报, 2008, 62(14): 147301.
7 Liu C M, Chen X R, Ji G F. First-principles investigations on structural, elastic and electronic properties of SnO_2 under pressure[J]. Comp Mater Sci, 2011, 50(4): 1571-1577.
8 Lei L, Li J, Luo G Q, *et al*.. Preparation and electrical properties of Tin dioxide ceramics doped with zine oxide and diantimony trioxide[J]. J Chin Ceram Soc, 2008, 36(s1): 43-47.
9 Guo Yuzhong, Wang Jianhua, Huang Ruian, *et al*.. Electrical and optical properties of transparent and conductive Sb-doped SnO_2 films[J]. Journal of Inorganic Materials, 2002, 17(1): 131-138.
郭玉忠, 王剑华, 黄瑞安, 等. 掺杂SnO_2透明导电薄膜电学及光学性能研究[J]. 无机材料学报, 2002, 17(1): 131-138.
10 Wang Yuheng, Ma Jing, Ji Feng, *et al*.. Preparation and photoluminescence characteristic of SnO B Sb Thin Films[J]. Chinese Journal of Semicondutors, 2005, 26(5): 922-926.
王玉恒, 马 瑾, 计 峰, 等. SnO_2B Sb薄膜的制备和光致发光性质[J]. 半导体学报, 2005, 26(5): 922-926.
11 Wang He, Wei Changping, Peng Chunjia, *et al*.. Preparation of SnO_2:Sb transparent conducting thin films and photoelectric properties[J]. Journal of Chinese Ceramic Society, 2012, 40(7): 945-949.
王 贺, 魏长平, 彭春佳, 等. SnO_2:Sb透明导电薄膜的制备及光电性能[J]. 硅酸盐学报, 2012, 40(7): 945-949.
12 Deng Z H, Yan J F, Zhang F C, *et al*.. First-principle calulation of effects of Sb doping on electrical conductivity of SnO_2 transparent film[J]. Acta Photonica Sinica, 2007, 36(s1): 110-115.
13 Kresse G, Furthmuller J. Efficiency of ab-initio total energy calculations for metals and semiconductors using a plane-wave basis set[J]. Comput Mater Sci, 1996, 6(1): 15-50.
14 Antonov V, Iordanova I. Density-functional study of the elastic properties of titanium nitride layers[J]. J Optoelectron Adv M, 2009, 11(10): 1475-1478.
15 Milman V, Winkler B, White J A, *et al*.. Electronic structure, properties, and phase stabilities of inorganic crystals: A pseudopotential plane-wavestudy[J]. Quantum Chem, 2000, 77(5): 895-910.
16 Thangaraju B. Structural and electrical studies on highly conducting spray deposited fluorine and antimony doped SnO_2 thin films from $SnCl_2$ precursor[J]. Thin Solid Films, 2002, 402(1-2): 71-78.
17 Zhang Fuchun, Deng Zhouhu, Yan Junfeng, *et al*.. First- principles calculation of electronic structure and optical properties of ZnO[J]. Acta Optica Sinica, 2006, 26(8): 1203-1209.
张富春, 邓周虎, 阎军锋, 等. ZnO电子结构与光学性质的第一性原理计算[J]. 光学学报, 2006, 26(8): 1203-1209.
18 Borges P D, Scolfaro L M R, Alves H W L, *et al*.. DFT study of the electronic, vibrational, and optical properties of SnO_2 [J]. Chem Acc, 2010, 126(1-2): 39-44.
19 Duan Manyi, Xu Ming, Zhou Haiping, *et al*.. Electronic structure and optical properties of ZnO doped with carbon[J]. Acta Phys Sin, 2008, 57(10): 6520-6525.
段满益, 徐 明, 周海平, 等. 碳掺杂ZnO的电子结构和光学性质[J]. 物理学报, 2008, 57(10): 6520-6525.
20 Hou Qingyu , Dong Hongying, Ma Wen, *et al*.. First-principle study on the effect of high Ga dopingon the optical band gap and the band-edge of opticalabsorption of ZnO[J]. Acta Phys Sin, 2013, 62(15): 157101.
侯清玉, 董红英, 马 文, 等. Ga高掺杂对ZnO的最小光学带隙和吸收带边影响的第一性原理研究[J]. 物理学报, 2013, 62 (15): 157101.
21 Rahman G, Victor M, Garcia S. Surface-induced magnetism in C-doped SnO_2[J]. Appl Phys Lett, 2010, 96: 052508.

栏目编辑：张浩佳